

Theoretical Analysis of Factors Controlling Pd-Catalyzed Decarboxylative Coupling of Carboxylic Acids with Olefins

Song-Lin Zhang,[†] Yao Fu,^{*,†} Rui Shang,[†] Qing-Xiang Guo,[†] and Lei Liu^{*,‡}

Departments of Chemistry, University of Science and Technology of China, Hefei 230026, China, and Tsinghua University, Beijing 100084, China

Received September 3, 2009; E-mail: fuyao@ustc.edu.cn; lliu@mail.tsinghua.edu.cn

Abstract: Transition-metal-catalyzed decarboxylative coupling presents a new and important direction in synthetic chemistry. Mechanistic studies on decarboxylative coupling not only improve the understanding of the newly discovered transformations, but also may have valuable implications for the development of more effective catalyst systems. In this work, a comprehensive theoretical study was conducted on the mechanism of Myers' Pd-catalyzed decarboxylative Heck reaction. The catalytic cycle was found to comprise four steps: decarboxylation, olefin insertion, β -hydride elimination, and catalyst regeneration. Decarboxylation was the rate-limiting step, and it proceeded through a dissociative pathway in which Pd(II) mediated the extrusion of CO₂ from an aromatic carboxylic acid to form a Pd(II)-aryl intermediate. Further analysis was conducted on the factors that might control the efficiency of Myers' decarboxylative Heck reaction. These factors included Pd salts, ligands, acid substrates, and metals. (1) Regarding Pd salts, PdCl₂ and PdBr₂ were worse catalysts than Pd(TFA)₂, because the exchange of Cl or Br by a carboxylate from Pd was thermodynamically unfavorable. (2) Regarding ligands, DMSO provided the best compromise between carboxyl exchange and decarboxylation. Phosphines and *N*-heterocarbenes disfavored decarboxylation because of their electron richness, whereas pyridine ligands disfavored carboxyl exchange. (3) Regarding acid substrates, a good correlation was observed between the energy barrier of R-COOH decarboxylation and the R-H acidity. Substituted benzoic acids showed deviation from the correlation because of the involvement of $\pi(\text{substituent})-\sigma(\text{C}_{\text{ipso}}-\text{Pd})$ interaction. (4) Regarding metals, Ni and Pt were worse catalysts than Pd because of the less favorable carboxyl exchange and/or DMSO removal steps in Ni and Pt catalysis.

1. Introduction

Transition-metal-catalyzed decarboxylative cross-coupling using carboxylic acids as aryl sources has received considerable attention recently.¹ Compared to conventional catalytic couplings² where expensive unstable organometallic reagents are often required, decarboxylative coupling utilizes readily available and stable carboxylic acids as substrates, thus precluding the need for preparation of sensitive organometallic reagents. An additional advantage is that decarboxylative coupling generates CO₂ without producing toxic metal halides.

Pioneering work by Nilsson showed that stoichiometric Cu promoted decarboxylative coupling of aromatic acids with ArI.³ Cohen et al. found that with phenanthroline ligand Cu(I) could mediate decarboxylation of aromatic acids, producing aryl-Cu that could be protonated to yield arenes.⁴ Recently, Goossen et al. discovered elegant protocols for the decarboxylative coupling

of benzoic acids with ArBr via a Cu/Pd bimetallic catalysis.⁵ Cu was used for decarboxylation to produce aryl-Cu. It transmetalates with aryl-Pd(II) generated from oxidative addition of ArBr to Pd(0), ending up with a bis-arylated Pd(II) species. Finally, reductive elimination gives the biaryl product. Goossen's reaction has been nicely extended to ArCl⁶ and ArOTf⁷ as the electrophiles. Moreover, α -oxo carboxylates could be transformed under the bimetallic catalysis to give aryl ketones through decarboxylative coupling.⁸

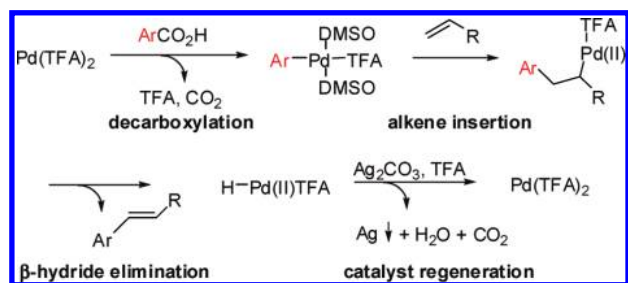
In addition to Cu, Pd by itself can also promote decarboxylative coupling. In 2002, Myers et al. discovered an interesting Heck-type reaction between aromatic acids and olefins catalyzed by Pd(TFA)₂ (TFA = CF₃CO₂⁻) (eq 1).⁹ Kinetic analysis indicated that decarboxylation was the rate-limiting step of the

[†] University of Science and Technology of China.

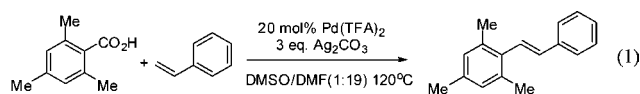
[‡] Tsinghua University.

- (1) (a) Baudoin, O. *Angew. Chem., Int. Ed.* **2007**, *46*, 1373. (b) Goossen, L. J.; Rodriguez, N.; Goossen, K. *Angew. Chem., Int. Ed.* **2008**, *47*, 3100.
- (2) *Metal-Catalyzed Cross-Coupling Reactions*; de Meijere, A., Diederich, F., Eds.; Wiley: Weinheim, Germany, 2004.
- (3) (a) Nilsson, M. *Acta Chem. Scand.* **1966**, *20*, 423. (b) Björklund, C.; Nilsson, M. *Acta Chem. Scand.* **1968**, *22*, 2585.
- (4) (a) Cohen, T.; Schambach, R. A. *J. Am. Chem. Soc.* **1970**, *92*, 3189. (b) Cohen, T.; Berninger, R. W.; Wood, J. T. *J. Org. Chem.* **1978**, *43*, 837.

- (5) (a) Goossen, L. J.; Deng, G.; Levy, L. M. *Science* **2006**, *313*, 662. (b) Goossen, L. J.; Rodriguez, N.; Melzer, B.; Linder, C.; Deng, G.; Levy, L. M. *J. Am. Chem. Soc.* **2007**, *129*, 4824. (c) Goossen, L. J.; Melzer, B. *J. Org. Chem.* **2007**, *72*, 7473. (d) Goossen, L. J.; Knauber, T. *J. Org. Chem.* **2008**, *73*, 8631.
- (6) Goossen, L. J.; Zimmermann, B.; Knauber, T. *Angew. Chem., Int. Ed.* **2008**, *47*, 7103.
- (7) Goossen, L. J.; Rodriguez, N.; Linder, C. *J. Am. Chem. Soc.* **2008**, *130*, 15248.
- (8) Goossen, L. J.; Rudolphi, F.; Ooppel, C.; Rodriguez, N. *Angew. Chem., Int. Ed.* **2008**, *47*, 3043.
- (9) (a) Myers, A. G.; Tanaka, D.; Mannion, M. R. *J. Am. Chem. Soc.* **2002**, *124*, 11250. (b) Tanaka, D.; Myers, A. G. *Org. Lett.* **2004**, *6*, 433. (c) For a recent improvement of the Myers reaction, see: Hu, P.; Kan, J.; Su, W.; Hong, M. *Org. Lett.* **2009**, *11*, 2341.

Scheme 1. Proposed Mechanism for Myers' Decarboxylative Cross-Coupling

catalytic cycle.¹⁰ The proposed aryl–Pd(II) intermediate from decarboxylation was captured and characterized by NMR and X-ray methods. This aryl–Pd(II) intermediate could undergo a facile, stoichiometric reaction with an olefin to yield the coupling product. On the basis of the results, a mechanism (Scheme 1) was proposed in which initial rate-limiting decarboxylation was followed by classical mechanistic steps of Heck reactions, i.e., olefin insertion, β -hydride elimination, and catalyst regeneration.



After Myers' pioneering work, Forgione et al. reported Pd-catalyzed decarboxylative coupling of heteroarene-carboxylic acids with ArBr.¹¹ Lee et al. reported Pd-catalyzed decarboxylative coupling of alkyne-carboxylic acids with ArBr.¹² Becht et al. reported Pd-catalyzed decarboxylative coupling of benzoic acids with Ar₂I⁺OTf⁻.¹³ Wu¹⁴ and Crabtree¹⁵ groups reported Pd-catalyzed decarboxylative coupling of cinnamyl acids and benzoic acids with ArI. In related studies, Tunge et al. developed novel methods for the substitution of allylic terminus via Pd-catalyzed intramolecular decarboxylative reaction of allyl carboxylic esters.¹⁶ Our own work in this area was the discovery of novel Pd(II)-catalyzed synthesis of aromatic esters through decarboxylative coupling of oxalate monoesters with aryl halides.¹⁷

Despite the remarkable advances and great contemporary interest in catalytic decarboxylative couplings, many mechanistic details of the decarboxylation process remain ambiguous. As to Cu-based systems, Goossen et al. recently performed DFT calculations to analyze Cu(I)(phenanthroline)-mediated decar-

boxylation of benzoic acids.¹⁸ On the other hand, almost no theoretical study has been conducted to understand the mechanistic details of Pd-catalyzed decarboxylative coupling. Only Myers' study provided some spectroscopic and crystallographic evidence for some intermediates in the proposed process.¹⁰ Even so, the structural and energetic details about how these intermediates transform to each other remain largely unknown.

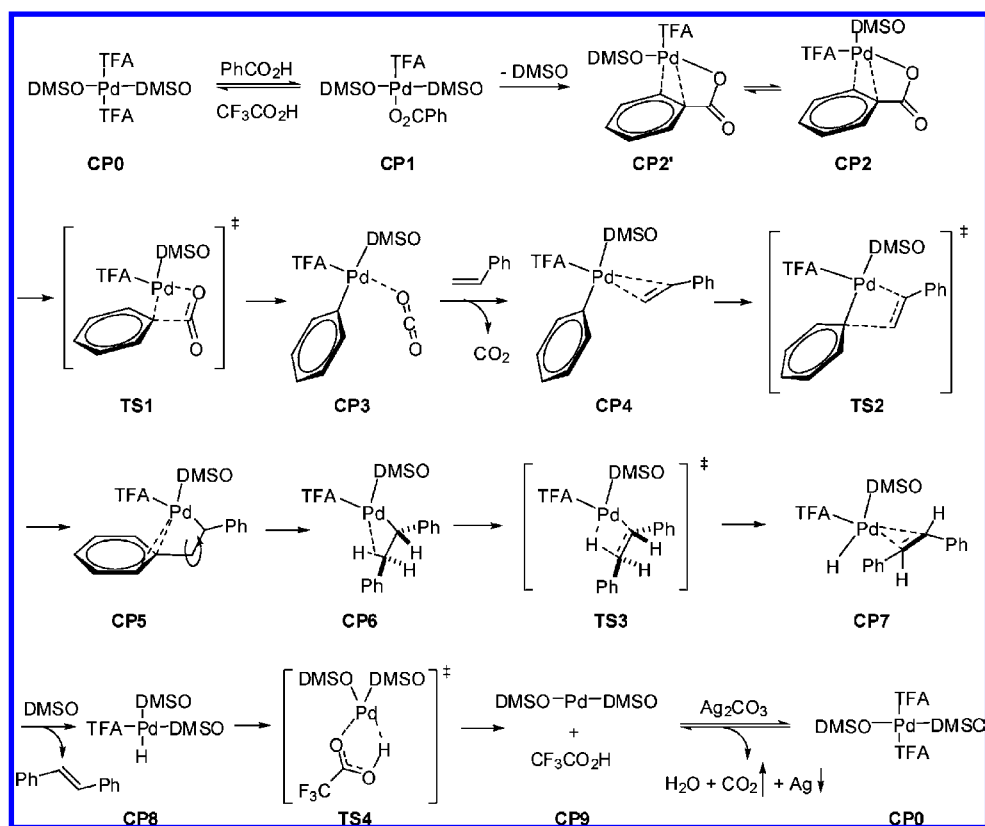
Here we report a thorough theoretical study on Pd-catalyzed decarboxylative couplings. Because Myers' decarboxylative Heck-type coupling stands for the best experimentally characterized system to date, we choose to focus on this particular reaction so that the calculation results can be compared to the experiment. Through the study we have obtained detailed structural and energetic information about each step of the decarboxylative coupling. More importantly, through systematic analysis of the catalysts, substrates, and ligands, the study sheds important insights into the various factors controlling the activation barrier of the decarboxylation process. These results may have valuable implications for the development of new, more effective catalyst systems for decarboxylative couplings.

2. Methods

All calculations were performed with Gaussian 03.¹⁹ B3LYP method was used.²⁰ Geometry optimization was conducted with the 631LAN basis set (i.e., Lan12dz for Ni, Pd, or Pt, and 6-31G(d) for the other elements).²¹ Frequency analysis was conducted at the same level of theory to verify the stationary points to be real minima or saddle points and to get the thermodynamic energy corrections. For each saddle point, the intrinsic reaction coordinate (IRC) analysis²² was carried out to confirm that it connected the correct reactant and product on the potential energy surface. Natural population analysis (NPA) was performed also at the same level of theory.²³ Single-point energy calculations were performed on the stationary points by using a larger basis set, i.e., SDD for Ni, Pd, or Pt and 6-311+G(d, p) for the other elements. Solvent effect (solvent = DMF) was calculated by using self-consistent reaction field method²⁴ with CPCM solvation model²⁵ and UAHF radii. Single-point energies corrected by Gibbs free energy corrections and solvation energies were used to describe the reaction energetics throughout the study.

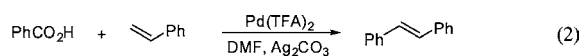
- (10) Tanaka, D.; Romeril, S. P.; Myers, A. G. *J. Am. Chem. Soc.* **2005**, *127*, 10323.
 (11) Forgione, P.; Brochu, M.-C.; St-Onge, M.; Thesen, K. H.; Bailey, M. D.; Bilodeau, F. *J. Am. Chem. Soc.* **2006**, *128*, 11350.
 (12) (a) Moon, J.; Jeong, M.; Nam, H.; Ju, J.; Moon, J. H.; Jung, H. M.; Lee, S. *Org. Lett.* **2008**, *10*, 945. (b) Moon, J.; Jang, M.; Lee, S. *J. Org. Chem.* **2009**, *74*, 1403.
 (13) (a) Becht, J.-M.; Le Drian, C. *Org. Lett.* **2008**, *10*, 3161. (b) Becht, J.-M.; Catala, C.; Le Drian, C.; Wagner, A. *Org. Lett.* **2007**, *9*, 1781.
 (14) (a) Wang, Z. Y.; Ding, Q. P.; He, X. D.; Wu, J. *Org. Biomol. Chem.* **2009**, *7*, 863. (b) Wang, Z. Y.; Ding, Q. P.; He, X. D.; Wu, J. *Tetrahedron* **2009**, *65*, 4635.
 (15) Voutchkova, A.; Coplin, A.; Leadbeater, N. E.; Crabtree, R. H. *Chem. Commun.* **2008**, 6312.
 (16) (a) Rayabarapu, D. K.; Tunge, J. A. *J. Am. Chem. Soc.* **2005**, *127*, 13510. (b) Burger, E. C.; Tunge, J. A. *J. Am. Chem. Soc.* **2006**, *128*, 10002. (c) Waetzig, S. R.; Rayabarapu, D. K.; Weaver, J. D.; Tunge, J. A. *Angew. Chem., Int. Ed.* **2006**, *45*, 4977. (d) Waetzig, S. R.; Tunge, J. A. *J. Am. Chem. Soc.* **2007**, *129*, 14860.
 (17) Shang, R.; Fu, Y.; Li, J. B.; Zhang, S. L.; Guo, Q. X.; Liu, L. *J. Am. Chem. Soc.* **2009**, *131*, 5738.

- (18) Goossen, L. J.; Thiel, W. R.; Rodriguez, N.; Linder, C.; Melzer, B. *Adv. Synth. Catal.* **2007**, *349*, 2241.
 (19) Frisch, M. J.; Trucks, G. W.; Schlegel, H. B.; et al. *Gaussian 03, revision D.01*; Gaussian, Inc.: Pittsburgh, PA, 2004.
 (20) Becke, A. D. *J. Chem. Phys.* **1993**, *98*, 5648.
 (21) Wadt, W. R.; Hay, P. J. *J. Chem. Phys.* **1985**, *82*, 299.
 (22) Gonzalez, C.; Schlegel, H. B. *J. Phys. Chem.* **1990**, *94*, 5523.
 (23) (a) Reed, A. E.; Weinstock, R. B.; Weinhold, F. *J. Chem. Phys.* **1985**, *83*, 735. (b) Glendening, E. D.; Reed, A. E.; Carpenter, J. E.; Weinhold, F. *NBO Version 3.1 in the Gaussian 98 Package*; University of Wisconsin: Madison, WI, 1990.
 (24) Cossi, M.; Rega, N.; Scalmani, G.; Barone, V. *J. Comput. Chem.* **2003**, *24*, 669.
 (25) Tomasi, J.; Mennucci, B.; Cammi, R. *Chem. Rev.* **2005**, *105*, 2999.
 (26) For recent reviews on Heck reactions, see: (a) Beletskaya, I. P.; Cheprakov, A. V. *Chem. Rev.* **2000**, *100*, 3009. (b) Dounay, A. B.; Overman, L. E. *Chem. Rev.* **2003**, *103*, 2945.
 (27) Some previous theoretical studies on Heck couplings and related Pd-catalyzed coupling reactions: (a) Deeth, R. J.; Smith, A.; Hii, K. K.; Brown, J. M. *Tetrahedron Lett.* **1998**, *39*, 3229. (b) Lin, B. L.; Liu, L.; Fu, Y.; Luo, S. W.; Chen, Q.; Guo, Q. X. *Organometallics* **2004**, *23*, 2114. (c) Deeth, R. J.; Smith, A.; Brown, J. M. *J. Am. Chem. Soc.* **2004**, *126*, 7144. (d) Kozuch, S.; Shaik, S. *J. Am. Chem. Soc.* **2006**, *128*, 3355. (e) Goossen, L. J.; Koley, D.; Hermmann, H. L.; Thiel, W. *Organometallics* **2005**, *24*, 2398. (f) Goossen, L. J.; Koley, D.; Hermann, H. L.; Thiel, W. *J. Am. Chem. Soc.* **2005**, *127*, 11102. (g) Goossen, L. J.; Koley, D.; Hermann, H. L.; Thiel, W. *Organometallics* **2006**, *25*, 54. (h) Surawatanawong, P.; Fan, Y.; Hall, M. B. *J. Organomet. Chem.* **2008**, *693*, 1552. (i) Surawatanawong, P.; Hall, M. B. *Organometallics* **2008**, *27*, 6222.

Scheme 2. Detailed Reaction Pathway for Myers' Decarboxylative Heck Reaction Supported by Current Theoretical Analysis (Dissociative Decarboxylation Pathway)

3. Catalytic Cycle of the Myers Reaction

The catalytic cycle of the model reaction between benzoic acid and styrene (eq 2) is proposed on the basis of Myers' study and the established mechanism for Pd-catalyzed Heck reaction (Scheme 2).^{26,27} There are four steps in the cycle: decarboxylation ($\text{CP0} \rightarrow \text{CP3}$), olefin insertion ($\text{CP4} \rightarrow \text{CP5}$), β -hydride elimination ($\text{CP6} \rightarrow \text{CP8}$), and catalyst regeneration ($\text{CP8} \rightarrow \text{CP0}$).



3.1. Decarboxylation. Decarboxylation starts with *trans*-(DMSO)₂Pd(TFA)₂ (**CP0**). This complex has three possible isomers depending on how the DMSO molecules are bound to Pd. Our calculations (in DMF) indicate that the bis-*S*-bound isomer (**CP0-ss**) is the least stable (+8.4 kcal/mol), whereas **CP0-os** (mono-*O*-mono-*S*-bound, +0.1 kcal/mol) and **CP0-oo** (bis-*O*-bound, +0.0 kcal/mol) are nearly isoenergetic. Thus, dynamic exchange between *S*- and *O*-bound forms^{28–30} must be considered at every stage of the decarboxylative coupling process. Furthermore, *trans*-(DMSO)₂Pd(TFA)₂ is found to be much more stable than its *cis* isomer by 3.4 kcal/mol. Note that the crystal structure of (DMSO)₂Pd(TFA)₂ also corresponds to

the *trans* isomer but it exists as the **CP0-os** isomer.³¹ The slight difference between the crystal and computational structures may be attributed to the crystal packing force.

CP0 undergoes carboxyl exchange with benzoic acid, producing intermediate **CP1**. The free energy change of this step is calculated to be +3.7 kcal/mol. Note that for **CP1** the bis-*O*-bound isomer (i.e., **CP1-oo**) is again the most stable (Figure 1). From **CP1-oo** (note that in the following discussion we will only mention the most stable isomer), either the associative or dissociative pathway can take place for the extrusion of CO₂. Both possibilities are examined as follows (Scheme 3).

Associative Pathway. In this pathway the two DMSO ligands remain attached to Pd during decarboxylation. Transition state **TS_{assoc-oo}** is successfully located in which the two DMSOs are both *O*-bound (Figure 1). The energy barrier for this step is +41.2 kcal/mol as calculated from **CP1-oo**. In **TS_{assoc-oo}**, the *C_{ipso}* atom of the phenyl ring, an O atom of the leaving CO₂, the O atom of one DMSO, and an O atom of TFA form the coordination plane (Figure 1). Our calculation indicates that it is energetically more favorable for DMSO instead of TFA to occupy the *trans* position of *C_{ipso}*. The immediate product after CO₂ removal is a four-coordinated Pd complex (**PD_{cis-os}**) with two DMSOs *cis* to each other. **PD_{cis-os}** is expected to transform to its more stable *trans*-isomer **PD_{trans-os}**. Note that Myers et al. obtained the crystal structure of the *trans*-aryl-Pd(II) trifluoroacetate intermediate carrying two DMSOs, which was also found to be a *trans* complex.¹⁰ However, in Myers' crystal the two DMSOs were both *S*-bound, whereas our calculations

(28) Some other examples for the use of DMSO as possible coordinating ligand in Pd-catalyzed processes include the following: (a) Larock, R. C.; Hightower, T. R. *J. Org. Chem.* **1993**, *58*, 5298. (b) Chen, M. S.; White, M. C. *J. Am. Chem. Soc.* **2004**, *126*, 1346. (c) Zhou, C.; Larock, R. C. *J. Am. Chem. Soc.* **2004**, *126*, 2302.

(29) (a) Steinhoff, B. A.; Fix, S. R.; Stahl, S. S. *J. Am. Chem. Soc.* **2002**, *124*, 766. (b) Steinhoff, B. A.; Stahl, S. S. *J. Am. Chem. Soc.* **2006**, *128*, 4348.

(30) Zierkiewicz, W.; Privalov, T. *Organometallics* **2005**, *24*, 6019.

(31) Bancroft, D. P.; Cotton, F. A.; Verbruggen, M. *Acta Crystallogr., Sect. C* **1989**, *45*, 1289.

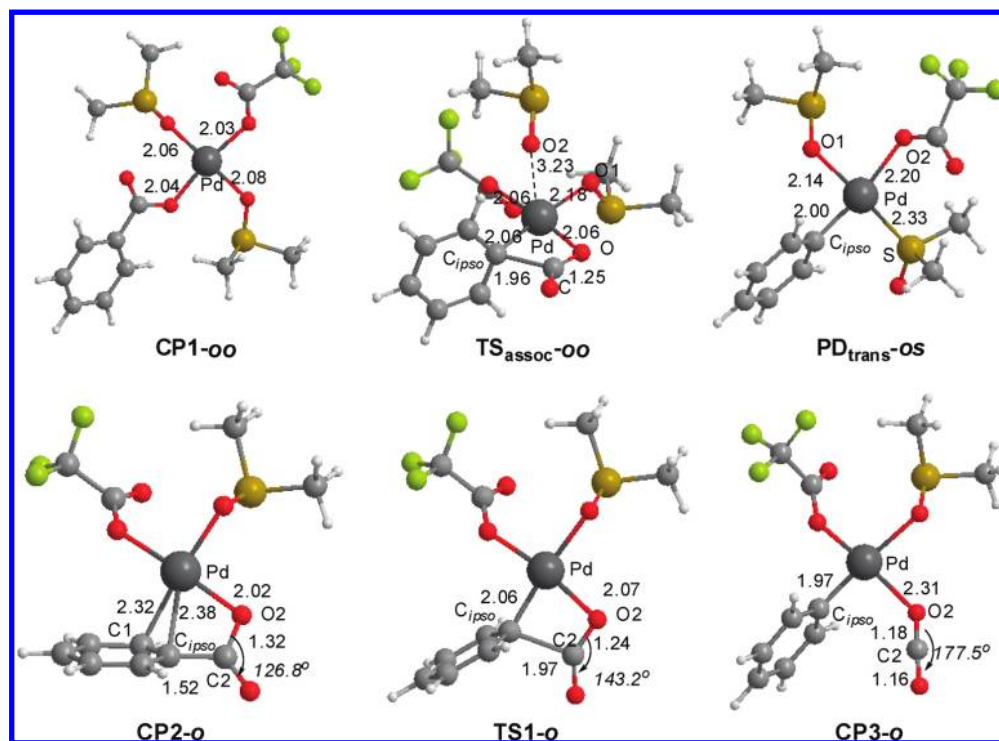
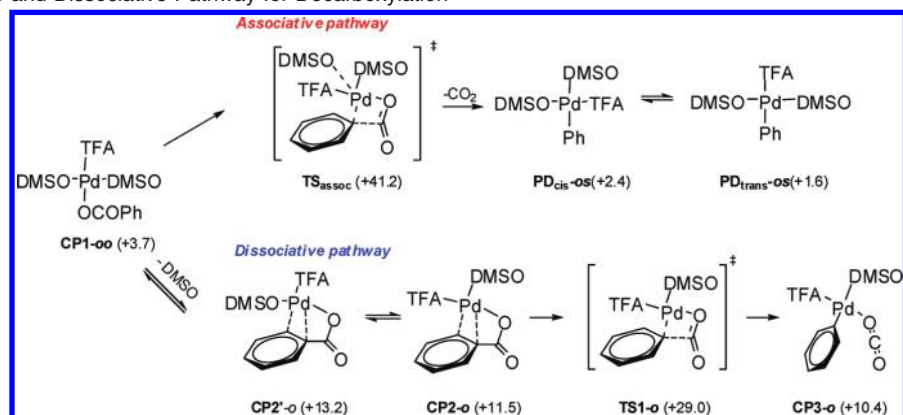


Figure 1. Key intermediates and transition states in associative and dissociative decarboxylation pathway.

Scheme 3. Associative and Dissociative Pathway for Decarboxylation^a



^a Values in parentheses are relative Gibbs free energies in DMF (kcal/mol).

indicate that **PD_{trans-os}** is more stable than **PD_{trans-ss}** by 1.8 kcal/mol in DMF.

Dissociative Pathway. In this pathway only one DMSO remains attached to Pd during decarboxylation. To do so, **CP1-oo** releases one DMSO, whose left position is immediately occupied by the phenyl ring of PhCO₂H through a η^2 binding mode. This process produces an active intermediate **CP2-o** and its isomer **CP2'-o** (Scheme 3). Both **CP2-o** and **CP2'-o** can extrude CO₂ through transition state **TS1-o** or **TS1'-o**. The structural difference between **TS1-o** and **TS1'-o** is whether the C_{ipso} atom is *trans* or *cis* to DMSO (Figure 1). Our calculation shows that **TS1'-o** is less stable than **TS1-o** by 1.8 kcal/mol in DMF. Therefore, dissociative decarboxylation should proceed through **TS1-o**. It is interesting to note that, in **TS1-o**, four atoms (i.e., Pd, C_{ipso}, C2, and O2) stay in the same plane that is perpendicular to the phenyl ring. This pathway has a relatively lower activation barrier of +29.0 kcal/mol. The immediate product of the dissociative decarboxylation is **CP3-o**, which can

exchange CO₂ with DMSO or PhCH=CH₂ to produce **PD_{trans-os}** or **CP4-o** respectively.

3.2. Olefin Insertion. Olefin insertion begins with **CP4-o** (Figure 2). **CP4-o** inserts the coordinated olefin into the aryl–Pd bond to produce **CP5-o** through a four-membered cyclic transition state **TS2-o**. The energy barrier for this step is +15.6 kcal/mol. In **CP4-o** the olefin is perpendicular to the Pd coordination plane, whereas in **TS2-o** the olefin lies in the Pd coordination plane. After olefin insertion, **CP5-o** isomerizes to **CP5-s** and becomes more stable by 1.3 kcal/mol. In **CP5-s**, the C_{ipso} atom remains coordinated to the Pd center. This observation is in agreement with Myers' crystal structure for a norbornene adduct of aryl–Pd(II)–TFA, which also turns out to be a S-bound complex with DMSO occupying the *trans* position of C_{ipso}.¹⁰ The Pd–C_{ipso} and Pd–C_α distances in Myers' crystal are 2.24 and 2.03 Å, as compared to 2.40 and 2.09 Å in **CP5-s**.

3.3. β -Hydride Elimination. To undergo β -hydride elimination, **CP5-s** rotates its phenyl group around the C_α–C_β bond

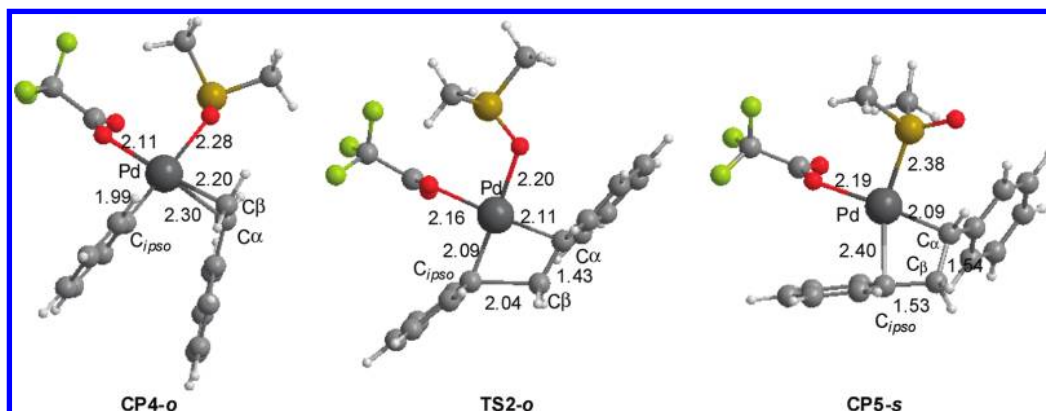


Figure 2. Key intermediates and transition state in olefin insertion.

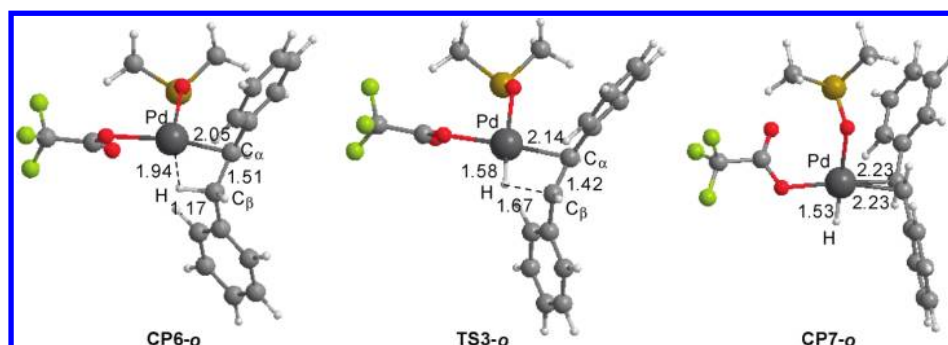


Figure 3. Key intermediates and transition state in β -hydride elimination.

so that one of the benzylic H atoms lies in the Pd–C α –C β plane. This gives intermediate **CP6-o**, featuring an agostic interaction of β -C–H to Pd center (Figure 3). From **CP6-o**, β -hydride elimination occurs to produce **CP7-o** through transition state **TS3-o**. The energy barrier for this step is only +5.4 kcal/mol as calculated from **CP5-s**. In both **TS3-o** and **CP7-o**, the hydride H occupies the *trans* position of DMSO. Furthermore, in **CP7-o** the olefin bond of stilbene is perpendicular to the coordination plane of Pd.

3.4. Catalyst Regeneration. In the last step, displacement of stilbene by DMSO releases the coupling product and generates a bis(DMSO)–Pd hydride **CP8-oo**. Then, the active catalyst (i.e., *trans*-**CP0-oo**) is regenerated from **CP8-oo**. This process has been recently studied by both experimental and computational methods.³² Two pathways have been proposed. One is the direct insertion pathway in which the oxidant directly inserts into the Pd–H bond to produce (X)Pd(II)–hydroperoxide. This intermediate is protonated by HX to give PdX₂ and hydroperoxide. The other one is the Pd(0) pathway, in which an initial reductive elimination of HX from Pd(H)(X) occurs to produce Pd(0) that is oxidized by the oxidant to become PdX₂. It has been shown that, for labile, monodentate ligands such as pyridine, the Pd(0) pathway is favored. Because in Myers' reaction the ligand is DMSO, we consider the Pd(0) pathway to be the favored one.³³

Our calculation shows that reductive elimination of CF₃COOH from **CP8-oo** has an activation barrier of +8.7 kcal/mol and is exothermic by –12.0 kcal/mol. Then, oxidation of Pd(0)(DMSO)₂ by Ag₂CO₃ in the presence of trifluoroacetic acid gives (DMSO)₂Pd(II)(TFA)₂. This oxidation is slightly endothermic by +1.5 kcal/mol. Overall, catalyst regeneration from **CP8-oo** to *trans*-**CP0-oo** is exothermic by –10.4 kcal/mol and, therefore, thermodynamically favorable.

3.5. Overall Catalytic Cycle and Rate-Limiting Step. Figure 4 shows the free energy profile for the catalytic cycle of Myers' decarboxylative Heck reaction. The part marked in blue describes the associative pathway, while the part in red describes the dissociative pathway. According to the profile, decarboxylation proceeds through the dissociative pathway with an activation barrier of +29.0 kcal/mol. Compared to decarboxylation, olefin insertion, β -hydride elimination, and catalyst regeneration are all facile steps. Thus, decarboxylation is the rate-determining step for Pd-catalyzed decarboxylative coupling of arenecarboxylic acids with alkenes.

4. Factors Controlling the Efficiency of Decarboxylative Coupling

In the catalytic cycle we identify that decarboxylation is the rate-determining step. In this part, the various factors controlling the decarboxylation step are discussed, which include the anionic ligand, the neutral ligand, substrate, and metal. As shown in Figure 4, the overall activation barrier for decarboxylation can be affected by the energy costs of three steps: (1) the energy required for carboxyl exchange (**CP0** \rightarrow **CP1**), (2) the energy required for dissociation of one DMSO from Pd (**CP1** \rightarrow **CP2**), and (3) the activation energy required for the extrusion of CO₂ (**CP2** \rightarrow **TS1**). To better understand why the decarboxylation efficiency changes

(32) For recent reviews on Pd oxidations, see: (a) Stahl, S. S. *Angew. Chem., Int. Ed.* **2004**, *43*, 3400. (b) Gligorich, K. M.; Sigman, M. S. *Angew. Chem., Int. Ed.* **2006**, *45*, 6612. (c) Piera, J.; Backvall, J.-E. *Angew. Chem., Int. Ed.* **2008**, *47*, 3506.

(33) For some recent studies on this subject, see: (a) Landis, C. R.; Morales, C. M.; Stahl, S. S. *J. Am. Chem. Soc.* **2004**, *126*, 16302. (b) Popp, B. V.; Stahl, S. S. *J. Am. Chem. Soc.* **2007**, *129*, 4410. (c) Konnick, M. M.; Stahl, S. S. *J. Am. Chem. Soc.* **2008**, *130*, 5753. (d) Keith, J. M.; Goddard, W. A., III. *J. Am. Chem. Soc.* **2009**, *131*, 1416. (e) Popp, B. V.; Stahl, S. S. *Chem.–Eur. J.* **2009**, *15*, 2915.

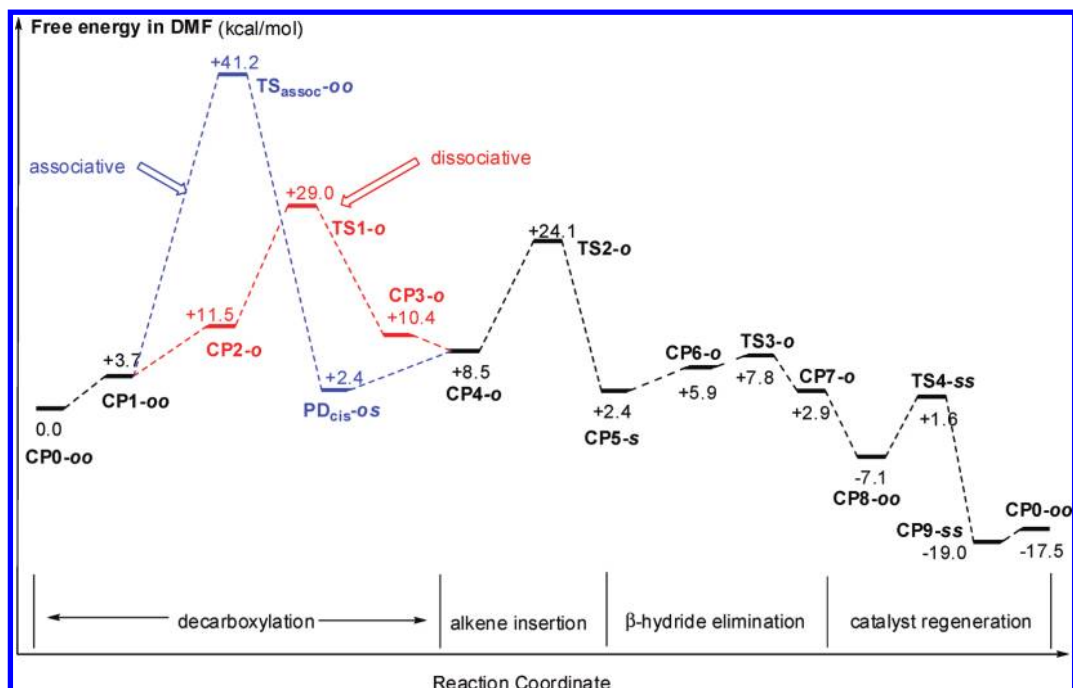


Figure 4. Free energy profile for the catalytic cycle of Myers' decarboxylative Heck reaction in DMF.

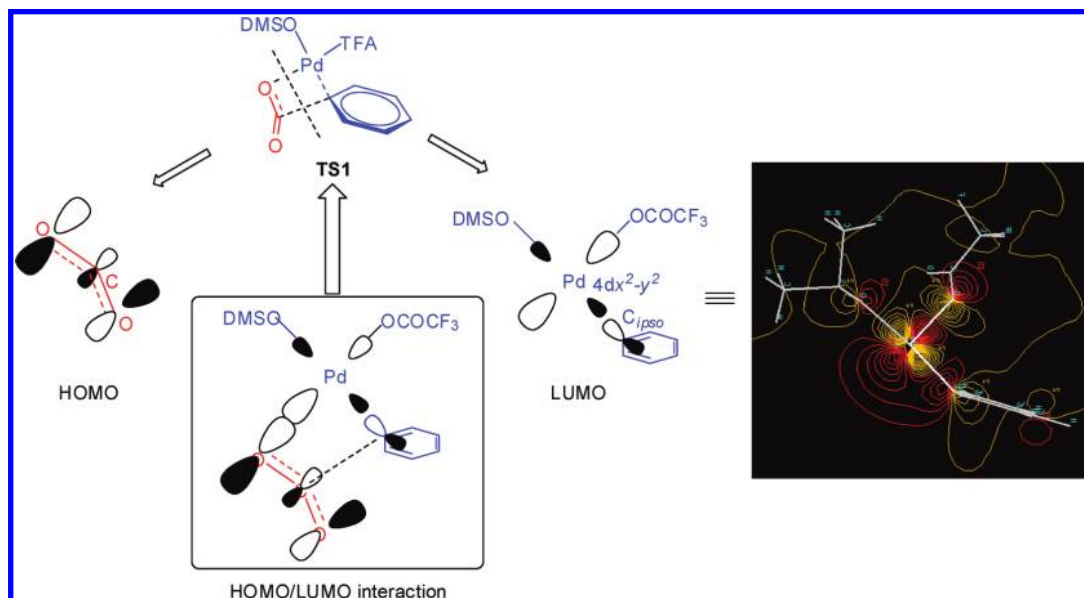


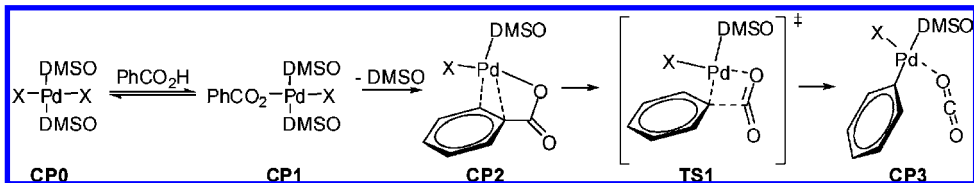
Figure 5. Fragment orbital analysis for TS1.

in different catalytic systems, the effect of each factor on the three steps is analyzed.

4.1. Orbital Analysis of the Decarboxylation Transition State. Before studying each factor, we analyze the orbital interactions for the extrusion of CO_2 from the Pd complex. Thus, we divide **TS1** into two fragments (Figure 5), i.e., $\text{Pd}(\text{DMSO})(\text{TFA})(\text{Ph})$ and the deformed CO_2 moiety.

Calculation shows that the LUMO of the $\text{Pd}(\text{DMSO})(\text{TFA})(\text{Ph})$ fragment is mainly composed of the Pd $4d_{x^2-y^2}$ orbital and some contribution from the $\sigma^*(\text{Pd}-\text{C}_{ipso})$ antibond. The Pd $4d_{x^2-y^2}$ orbital is highly asymmetric presumably due to the stronger *trans* influence of the anionic TFA group than the neutral DMSO. The HOMO of the deformed CO_2 is a π bond. It overlaps with the LUMO of $\text{Pd}(\text{DMSO})(\text{TFA})(\text{Ph})$ in the manner shown in Figure 5.

From the orbital interactions we can draw the following conclusions. First, an electron-deficient Pd center leads to a low-lying LUMO orbital that can interact more strongly with the π bond of deformed CO_2 . Thus, electron-deficient ligands, rather than electron-rich ones, are expected to facilitate decarboxylation. Second, anionic ligands with a stronger *trans* influence can stabilize the decarboxylation transition state because a stronger desymmetrization of the Pd $4d_{x^2-y^2}$ orbital can bring about a more favorable HOMO/LUMO interaction. Third, from the precomplex **CP2** to **TS1**, the NPA charge on the C_{ipso} atom changes from -0.168 to -0.319 while the NPA charge on the carboxyl carbon increases from $+0.814$ to $+0.934$. Thus, any factor that stabilizes the accumulating negative charges on C_{ipso} or the positive charge on the carboxyl carbon can contribute to the stabilization of **TS1**,

Table 1. Effect of Anionic Ligands on the Decarboxylation Step (kcal/mol)


X	$\Delta G(\text{CP0} \rightarrow \text{CP1})$	$\Delta G(\text{CP1} \rightarrow \text{CP2})$	$\Delta G^\ddagger(\text{CP2} \rightarrow \text{TS1})$	$\Delta G^\ddagger_{\text{decarboxylation}}^a$
TFA	3.7	7.8	17.5	+29.0
Cl	20.4	4.3	15.7	+40.4
Br	23.2	4.2	15.4	+42.8

$$^a \Delta G^\ddagger_{\text{decarboxylation}} = \Delta G(\text{CP0} \rightarrow \text{CP1}) + \Delta G(\text{CP1} \rightarrow \text{CP2}) + \Delta G^\ddagger(\text{CP2} \rightarrow \text{TS1}).$$

facilitating the decarboxylation. These conclusions can be used to explain the calculation results as discussed below.

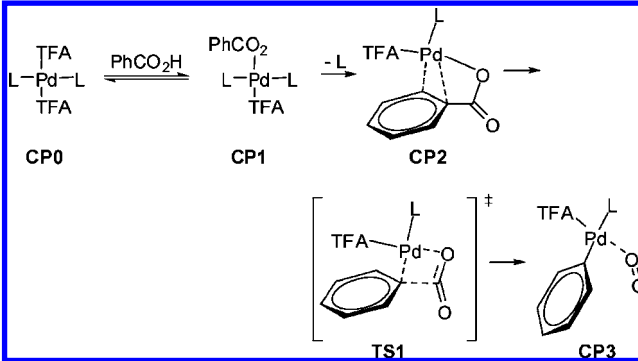
4.2. Effect of Anionic Ligands on Decarboxylation. Myers and co-workers found that trifluoroacetate played a key role in the decarboxylative palladation reaction, because other Pd salts such as PdCl₂ and PdBr₂ were ineffective or gave inferior results.¹⁰ Moreover, added bromide completely inhibited decarboxylation.¹⁰ To understand these observations, PdCl₂ and PdBr₂ are examined to evaluate the effect of anionic ligands on decarboxylation (Table 1).

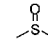
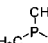
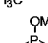
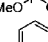
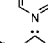
According to the orbital analysis, the anionic ligand with a stronger *trans* influence can stabilize the transition state of decarboxylation (namely, **TS1**). Indeed, the $\Delta G^\ddagger(\text{CP2} \rightarrow \text{TS1})$ values for Cl and Br are lower than that for TFA by ca. 2–3 kcal/mol, because Cl and Br exert a stronger *trans* influence than TFA. However, it is found that, in the carboxyl exchange step, the $\Delta G(\text{CP0} \rightarrow \text{CP1})$ value is only +3.7 kcal/mol for TFA, as compared to +20.4 and +23.2 kcal/mol for Cl and Br. Consequently, the overall activation barrier of decarboxylation is very high (over +40 kcal/mol) for PdCl₂ and PdBr₂. This explains why PdCl₂ and PdBr₂ provided inferior results in decarboxylation.

4.3. Effect of Neutral Ligand on Decarboxylation. Several common types of neutral ligands including phosphine, phosphite, pyridine, and *N*-heterocarbene are examined for their effects on the decarboxylation step (Table 2). It is found, not without surprise, that DMSO gives the lowest activation barrier as compared to all the above popular ligands. This calculation result is in agreement with the experimental observation that DMSO is thus far the only appropriate ligand system for the decarboxylative Heck reaction.^{9,10}

A phosphine or phosphite ligand (e.g., PMe₃ or P(OMe)₃) is found to be detrimental to decarboxylation as reflected by the high activation barriers. The reason is 2-fold: (1) Phosphine or phosphite ligands are relatively electron-rich and, therefore, generate a less electron-deficient Pd(II) center. This would increase the energy cost for the extrusion of CO₂ in the transition from **CP2** to **TS1** (27.5 kcal/mol for PMe₃ and 26.1 kcal/mol for P(OMe)₃, vs 17.5 kcal/mol for DMSO). (2) Phosphine and phosphite ligands coordinate to Pd more strongly, so that the ligand dissociation (i.e., **CP1** → **CP2**) also becomes highly unfavorable (13.9 kcal/mol for PMe₃ and 10.4 kcal/mol for P(OMe)₃, vs 7.8 kcal/mol for DMSO).

Compared to phosphine and phosphite, pyridine is less electron-rich, and it does not coordinate to Pd very strongly. In agreement with this argument, we find that the energy costs of the ligand dissociation (**CP1** → **CP2**) and CO₂ extrusion (**CP2** → **TS1**) steps are relatively low for pyridine (8.9 and 19.0 kcal/mol, vs 7.8 and 17.5 kcal/mol for DMSO). However, it is found that the energy cost of the carboxyl exchange step (**CP0** → **CP1**) is fairly high

Table 2. Effect of Neutral Ligand on Decarboxylation of PhCOOH (kcal/mol)^a


L	$\Delta G(\text{CP0} \rightarrow \text{CP1})$	$\Delta G(\text{CP1} \rightarrow \text{CP2})$	$\Delta G^\ddagger(\text{CP2} \rightarrow \text{TS1})$	$\Delta G^\ddagger_{\text{decarboxylation}}^a$
	3.7	7.8	17.5	+29.0
	7.0	13.9	27.5	+48.4
	5.4	10.4	26.1	+41.9
	10.2	8.9	19.0	+38.1
	11.0	24.5	26.7	+62.2

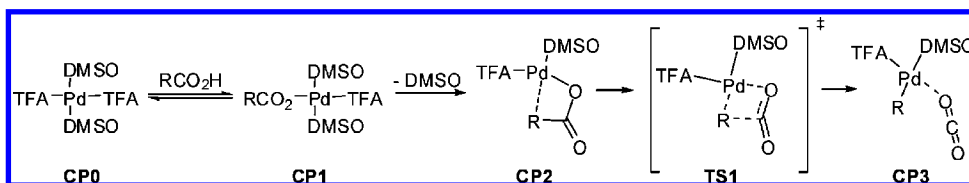
$$^a \Delta G^\ddagger_{\text{decarboxylation}} = \Delta G(\text{CP0} \rightarrow \text{CP1}) + \Delta G(\text{CP1} \rightarrow \text{CP2}) + \Delta G^\ddagger(\text{CP2} \rightarrow \text{TS1}).$$

for pyridine (10.2 kcal/mol vs 3.7 kcal/mol for DMSO). As a result, pyridine has a much higher activation barrier of decarboxylation than DMSO.

Finally, an *N*-heterocarbene ligand is found to be most unfavorable for Pd-mediated decarboxylation. Its electron richness and its strong coordination ability to Pd lead to very high energy costs for the ligand dissociation (**CP1** → **CP2**, 24.5 kcal/mol) and CO₂ extrusion (**CP2** → **TS1**, 26.7 kcal/mol) steps. Besides, it also has a high energy cost for the carboxyl exchange step (**CP0** → **CP1**, 11.0 kcal/mol).

4.4. Effect of Carboxylic Acid Substrates on Decarboxylation.

A number of carboxylic acids are examined to study the effect of substrates on decarboxylation. According to the results in Table 3, the following predictions can be made. First, alkynecarboxylic acids can undergo facile decarboxylation as indicated by the low activation barrier of propynecarboxylic acid (+16.3 kcal/mol). This prediction is supported by the study of Lee,¹² who showed that alkynecarboxylic acids could be decarboxylated to react with electrophiles under mild conditions. Second, Pd-mediated decarboxylation of vinyl carboxylic acids is also a feasible process because its activation barrier is only +26.5 kcal/mol. Third, alkanecarboxylic acids are probably not going to be useful in Pd-catalyzed decarboxylative couplings because of the very high

Table 3. Carboxylic Acid Substrate Effect on the Decarboxylation Step (kcal/mol)

Acid	$\Delta G(\text{CP0} \rightarrow \text{CP1})$	$\Delta G(\text{CP1} \rightarrow \text{CP2})$	$\Delta G^\ddagger(\text{CP2} \rightarrow \text{TS1})$	$\Delta G^\ddagger_{\text{decarboxylation}}^a$	Gas-phase acidity ^b
	3.7	7.8	17.5	+29.0	400.1
	1.3	14.7	14.7	+30.7	382.4
	5.3	6.7	13.6	+25.6	401.7
	4.1	7.3	13.8	+25.2	380.6
	8.2	0.7	13.5	+22.4	397.8
	3.4	5.1	11.2	+19.7	391.2
	7.4	-2.1	14.9	+20.2	396.7
CH ₃ -COOH	10.1	9.5	15.1	+34.7	415.9
C ₂ H ₅ -COOH	11.9	8.5	18.2	+38.6	418.0
	11.0	5.7	16.3	+33.0	413.2
CH ₂ =CH-COOH	10.9	-11.4	26.5	+26.5	407.8
HC≡C-COOH	4.6	-1.4	13.1	+16.3	376.1

^a $\Delta G^\ddagger_{\text{decarboxylation}} = \Delta G(\text{CP0} \rightarrow \text{CP1}) + \Delta G(\text{CP1} \rightarrow \text{CP2}) + \Delta G^\ddagger(\text{CP2} \rightarrow \text{TS1})$. ^b Gas phase acidity of the C_{ipso}-H bond of the hydrocarbon compound that is generated after decarboxylation of the carboxylic acid, see also ref 34.

activation barriers (over +33 kcal/mol) and the propensity of alkyl-Pd to undergo side reactions.

The above results appear to indicate that the activation barrier of Pd-mediated decarboxylation of RCOOH should correlate with the acidity of the R-H bond. Specifically, a more acidic R-H bond should be associated with a more readily decomposable R-COOH. This speculation is largely correct as shown by the plot of the decarboxylation barriers against the gas phase acidities of the C_{ipso}-H bonds (Figure 6). The finding is important because it implies that transition-metal-mediated decarboxylation and C-H bond activation may share some common features.

Despite the above correlation, it is surprising to notice that benzoic acids with electron-withdrawing substituents dramatically deviate from the correlation line (Figure 6). In fact, an electron-donating group (e.g., OMe) reduces the activation barrier of decarboxylation whereas an electron-withdrawing substituent (e.g., NO₂) does the opposite. This theoretical prediction is in agreement with the experiment, where electron-rich benzoic acids were also found to be better substrates in the decarboxylative couplings.^{9,10}

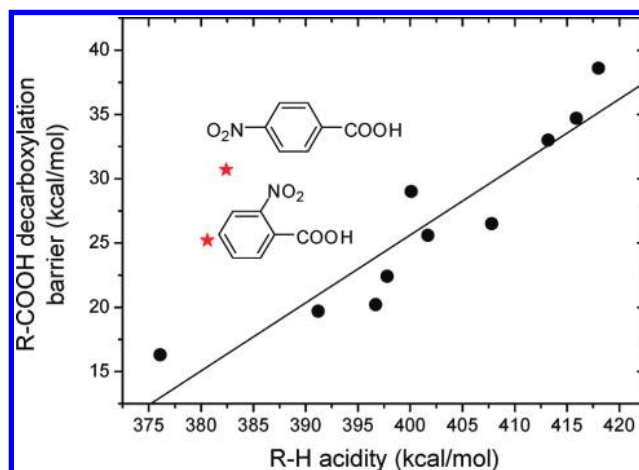


Figure 6. Correlation between the activation barrier of Pd-mediated decarboxylation of RCOOH and the acidity of the R-H bond.

Detailed analysis indicates that the problem stems from the DMSO removal step (i.e., CP1 → CP2). For instance, for 4-NO₂-C₆H₄COOH the removal of a DMSO from CP1 to generate CP2 costs +14.7 kcal/mol, whereas the same process only costs +6.7 kcal/mol for 4-OMe-C₆H₄COOH. The large difference between the two acids can be explained by the formation of the C_{ipso}-Pd(II) bond in CP2. Specifically, a 4-NO₂ group (as a π acceptor) should

(34) C-H acidities in Table 3 are theoretical values at the B3LYP/6-311+G(d,p) level. These theoretical values are found to reproduce the available experimental data fairly well: (a) Romer, B.; Gatev, G. G.; Zhong, M.; Brauman, J. I. *J. Am. Chem. Soc.* **1998**, *120*, 2919. (b) Fattahi, A.; McCarthy, R. E.; Ahmad, M. R.; Kass, S. R. *J. Am. Chem. Soc.* **2003**, *125*, 11746, and references cited therein.

Table 4. Metal Center Effect on the Decarboxylation Step (kcal/mol)^a

metal	$\Delta G(\text{CP0} \rightarrow \text{CP1})$	$\Delta G(\text{CP1} \rightarrow \text{CP2})$	$\Delta G^\ddagger(\text{CP2} \rightarrow \text{TS1})$	$\Delta G^\ddagger_{\text{decarboxylation}}$
Ni	10.0	13.6	19.9	+43.5
Pd	3.7	7.8	17.5	+29.0
Pt	9.7	8.4	16.5	+34.6

$$^a \Delta G^\ddagger_{\text{decarboxylation}} = \Delta G(\text{CP0} \rightarrow \text{CP1}) + \Delta G(\text{CP1} \rightarrow \text{CP2}) + \Delta G^\ddagger(\text{CP2} \rightarrow \text{TS1}).$$

destabilize the $C_{\text{ipso}}-\text{Pd}(\text{II})$ bond that is perpendicular to the phenyl ring (see Figure 1), but this $\pi(\text{NO}_2)-\sigma(\text{C}-\text{Pd})$ type of interaction does not play any role in determining the R–H acidity (because the R–H bond is *not* perpendicular to the phenyl ring). As a result, substituted benzoic acids do not rigorously follow the correlation in Figure 6.

Furthermore, it is interesting to observe that the activation barrier of the 4-OMe-substituted benzoic acid (+25.6 kcal/mol) is about 3 kcal/mol higher than that for 2-OMe-substituted benzoic acid (+22.4 kcal/mol). Similarly, the activation barrier of the 4-NO₂-substituted benzoic acid (+30.7 kcal/mol) is about 5 kcal/mol higher than that for 2-NO₂-substituted benzoic acid (+25.2 kcal/mol). These observations indicate that the *ortho* substituents influence the reactivity of benzoic acids more via their influence on the σ electron density than the π electron density. Similar effects were reported by Goossen and Thiel in their study on Cu-catalyzed decarboxylation.¹⁸ This effect also explains why 2-furancarboxylic acid has a very low activation barrier for decarboxylation as compared to benzoic acid.

4.5. Metal Center Effect on Decarboxylation. All the d¹⁰ group elements (Ni, Pd, and Pt) are examined for the decarboxylation process. According to the results in Table 4, the overall activation barrier for the extrusion of CO₂ from benzoic acid follows the following order: Pd < Pt < Ni. As to Ni catalyst, it is found that the energy cost for the CO₂ extrusion step (CP2 → TS1, +19.9 kcal/mol) is only 2.4 kcal/mol higher than the Pd case. However, carboxyl exchange (CP0 → CP1) and removal of one DMSO (CP1 → CP2) cost a considerable amount of free energy for Ni. As to Pt, the energy cost for the decarboxylation step (CP2 → TS1, +16.5 kcal/mol) is even 1.0 kcal/mol lower than the Pd case. Unfortunately, the energy cost for the carboxyl exchange step (CP0 → CP1) is fairly high for the Pt catalyst. One may propose that the unfavorable effects of carboxyl exchange and DMSO removal steps in Ni- and Pt-catalyzed decarboxylation could be overcome by changing the ligands. It remains interesting to see whether Ni- and Pt-catalyzed decarboxylative cross-coupling could be accomplished experimentally.

5. Conclusions

Transition-metal-catalyzed decarboxylative cross-coupling uses readily available carboxylic acids to replace unstable organometallic reagents. This method presents a new and important direction in

synthetic organic chemistry. In the present work, we report the first comprehensive theoretical study on the mechanism of Pd-catalyzed decarboxylative Heck reaction discovered by Myers and co-workers. It is found that the overall catalytic cycle is composed of four steps: decarboxylation, olefin insertion, β -hydride elimination, and catalyst regeneration. Decarboxylation is concluded to be the rate-limiting step, in which Pd(II) mediates the extrusion of CO₂ from an aromatic carboxylic acid to form a Pd(II)–aryl intermediate. The dissociative pathway is favored in decarboxylation, so that dissociation of one DMSO ligand must take place prior to the extrusion of CO₂.

Further analysis on the various factors that may control the efficiency of Pd-catalyzed decarboxylative Heck reactions yields the following conclusions. First, PdCl₂ and PdBr₂ are much worse catalysts than Pd(TFA)₂, because the exchange of Cl or Br in a Pd complex with the carboxylate substrate is a highly unfavorable step in thermodynamics. Second, DMSO presents the best compromise between the carboxyl exchange and decarboxylation steps. Phosphine and *N*-heterocarbene ligands disfavor the decarboxylation step because of their electron richness. Pyridine-type ligands, on the other hand, disfavor the carboxyl exchange step. Third, there is a good correlation between the activation barrier of R–COOH decarboxylation and the acidity of the R–H bond. A more acidic R–H bond causes a more readily decomposable R–COOH. However, substituted benzoic acids show deviation from the correlation because of the involvement of $\pi(\text{substituent})-\sigma(C_{\text{ipso}}-\text{Pd})$ interaction. Finally, Ni and Pt are worse catalysts than Pd for decarboxylation because of the less favorable carboxyl exchange and/or DMSO removal steps in Ni and Pt catalysis. These results should also have valuable implications for other transition-metal-catalyzed decarboxylative reactions.

Acknowledgment. This study was supported by the National Natural Science Foundation of China (Nos. 20832004, 20802040, 20972148), the Specialized Research Fund for the Doctoral Program of Higher Education (No. 200800030074), and the NCET (080519).

Supporting Information Available: Detailed optimized geometries, free energies, thermal corrections. Discussion on the binding mode of DMSO. Full citation of ref 19. This material is available free of charge via the Internet at <http://pubs.acs.org>.

JA907448T